

Electronic Supplementary Information

Substitution Effect on Carbazole-centered Donors for Tuning Exciplex Systems as Cohost for Highly Efficient Yellow and Red OLEDs

Li-Ming Chen^a, I-Hung Lin^b, Yu-Chi You^a, Wei-Chih Wei^a, Meng-Ju Tsai^a, Wen-Yi
Hung^{*, b}, Ken-Tsung Wong^{*, a, c}

^aDepartment of Chemistry, National Taiwan University, Taipei, 10617, Taiwan

^bDepartment of Optoelectronics and Materials Technology, National Taiwan Ocean
University, Keelung 202, Taiwan

^cInstitute of Atomic and Molecular Science, Academia Sinica, Taipei, 10617, Taiwan

E-mail: wenhung@mail.ntou.edu.tw; kenwong@ntu.edu.tw

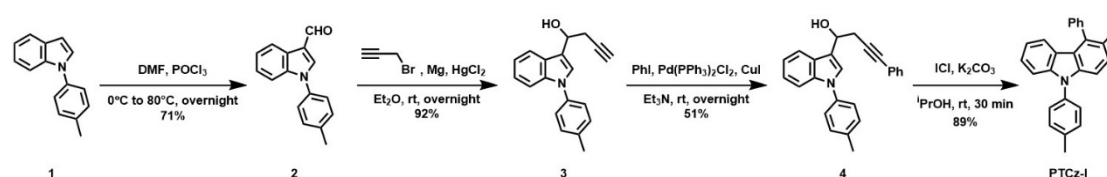
| Contents | Page |
|----------------------|---|
| Experimental section | S4 |
| Figure S1 | Cyclic voltammograms of PTCz-9'Cz, PTCz-3'TCz, and PTCz-NTol ₂ . S10 |
| Figure S2 | HOMO energy levels of (a) PTCz-9'Cz, (b) PTCz-3'TCz and (c) PTCz-NTol ₂ determined by photoelectron yield spectroscopy (Riken AC-2). S10 |
| Figure S3 | Room temperature absorption (UV-Vis), emission (PL) and Phosphorescence (Phos) spectra of (a) PTCz-9'Cz, (b) PTCz-3'TCz, and (c) PTCz-NTol ₂ neat films. S11 |
| Figure S4 | (a)-(c) Transient PL decays and (d)-(f) PL spectra of Donor:PO-T2T (1:1) blend films at room temperature. S11 |
| Figure S5 | Plots of (a) J-V-L characteristics, (b) correlation profile of luminance with EQE and power efficiency (PE), and (c) normalized EL spectra for PTCz-9'Cz:PO-T2T devices with different donor-acceptor ratios. S11 |
| Figure S6 | Plots of (a) J-V-L characteristics, (b) correlation profile of luminance with EQE and power efficiency (PE), and (c) normalized EL spectra for PTCz-3'TCz:PO-T2T devices with different donor-acceptor ratios. S12 |
| Figure S7 | Plots of (a) J-V-L characteristics, (b) correlation profile of luminance with EQE and power efficiency (PE), and (c) normalized EL spectra for PTCz-NTol ₂ :PO-T2T devices with different donor-acceptor ratios. S12 |
| Figure S8 | (a) Room temperature absorption (UV-Vis) and emission (PL) spectra of iCzPNT and iCzBTh2CN in toluene solution and (b) cyclic voltammograms of iCzPNT and iCzBTh2CN. The cyclic voltammogram of iCzPNT was obtained despite poor solubility in CH ₂ Cl ₂ . S13 |
| Figure S9 | Room temperature absorption (UV-Vis) and emission (PL) spectra of PTCz-9'Cz:PO-T2T (2:1) blend films with 10 wt%-doped (a) iCzPNT and (c) iCzBTh2CN at room temperature and transient PL decays of PTCz-9'Cz:PO-T2T (2:1) blend films with 10 wt%-doped (b) iCzPNT and (d) iCzBTh2CN at room temperature. S13 |
| Table S1 | Theoretical calculations of PTCz-based donor (a) LUMO (b) HOMO and (c) ground state geometry at the B3LYP/6-31+G(d,p) level S14 |
| Table S2 | Theoretical calculations of TCz-based donor (a) LUMO (b) HOMO and (c) ground state geometry at the B3LYP/6-31+G(d,p) level S15 |
| Table S3 | Physical properties of iCzPNT and iCzBTh2CN. S15 |
| Figure S10 | ¹ H NMR spectrum of 3. S16 |
| Figure S11 | ¹³ C NMR spectrum of 3. S16 |
| Figure S12 | ¹ H NMR spectrum of 4. S17 |

| | | |
|------------|--|-----|
| Figure S13 | ^{13}C NMR spectrum of 4. | S17 |
| Figure S14 | ^1H NMR spectrum of PTCz-I. | S18 |
| Figure S15 | ^{13}C NMR spectrum of PTCz-I. | S18 |
| Figure S16 | ^1H NMR spectrum of PTCz-9'Cz. | S19 |
| Figure S17 | ^{13}C NMR spectrum of PTCz-9'Cz. | S19 |
| Figure S18 | ^1H NMR spectrum of PTCz-3'TCz. | S20 |
| Figure S19 | ^{13}C NMR spectrum of PTCz-3'TCz. | S20 |
| Figure S20 | ^1H NMR spectrum of PTCz-NTol ₂ . | S21 |
| Figure S21 | ^{13}C NMR spectrum of PTCz-NTol ₂ . | S21 |
| Figure S22 | ^1H NMR spectrum of iCzPNT. | S22 |
| Figure S23 | ^1H NMR spectrum of iCzBTh2CN. | S22 |
| Figure S24 | ^{13}C NMR spectrum of iCzBTh2CN. | S23 |

Experimental Section

Materials

All the chemicals and reagents were used without purification from commercial sources. Solvents for chemical analyses and reactions were purified by distillation with drying equipment before use. 1-(*p*-tolyl)-1*H*-indole (1)¹, 1-(*p*-tolyl)-1*H*-indole-3-carbaldehyde (2)², 3-(4,4,5,5-tetramethyl-1,3,2-dioxaborolan-2-yl)-9-(*p*-tolyl)-9*H*-carbazole³, 5,10-dibromonaphtho[1,2-*c*:5,6-*c'*]bis([1,2,5]thiadiazole)⁴, 1,3-dibromobenzo[*c*]thiophene-5,6-dicarbonitrile⁵, and PO-T2T⁶ were prepared according to existing literatures.



Scheme S1 Synthetic pathway for PTCz-I.

Synthesis of 1-(1-(*p*-tolyl)-1*H*-indol-3-yl)-3-butyn-1-ol (3)

To a double-necked flask was added a mixture of magnesium powder (2.95 g, 123 mmol) and mercury(II) chloride (0.27 g, 1.0 mmol). The system was flame-dried, flushed with argon, and added anhydrous diethyl ether (200 mL). A portion of propargyl bromide (80 wt% in toluene, 16.15 mL, 145 mmol) in anhydrous diethyl ether (70 mL) was initially added to initiate the reaction. After the solution started to bubble and became turbid, the rest of the propargyl bromide solution was added dropwise to the mixture and stirred at room temperature for an hour. Subsequently, the mixture was cooled to 0 °C with an ice bath and added dropwise 2 (19.0 g, 80.8 mmol) in anhydrous THF (70 mL) via syringe. The solution was then stirred at room temperature overnight under an argon atmosphere. The resulting mixture was quenched by addition of water, passed through a celite pad, extracted with ethyl acetate and brine. The combined organic phase was dried with MgSO₄ and concentrated through rotary evaporation. The crude product was ultimately purified with column chromatography on silica gel (ethyl acetate/hexane = 1:3) to give the title compound 3 as a yellow oil (20.56 g, 75 mmol, 92%). ¹H NMR (400 MHz, CDCl₃) δ 7.79 (dt, *J* = 7.6, 0.9 Hz, 1H), 7.55 – 7.48 (m, 1H), 7.41 – 7.34 (m, 3H), 7.32 (d, *J* = 8.5 Hz, 2H), 7.25 – 7.14 (m, 2H), 5.29 (t, *J* = 6.2 Hz, 1H), 2.91 (dd, *J* = 6.3, 2.6 Hz, 2H), 2.44 (s, 3H), 2.40 (s, 1H), 2.13 (t, *J* = 2.6 Hz, 1H). ¹³C NMR (101 MHz, CDCl₃) δ 136.90, 136.52, 136.50, 130.16, 126.74, 125.30, 124.31, 122.68, 120.28, 119.65, 118.31, 110.78, 81.21, 71.00, 66.72, 66.60, 28.11, 21.03. HRMS (*m/z*, MALDI, [M-OH]⁺) calcd for C₁₉H₁₇NO 258.1283 found 258.1481.

Synthesis of 4-phenyl-1-(1-(*p*-tolyl)-1*H*-indol-3-yl)-3-butyn-1-ol (4)

To a double-necked flask was added a mixture of 3 (20.56 g, 75 mmol), bis(triphenylphosphine)palladium chloride (524 mg, 0.75 mmol) and copper(I) iodide (284.4 mg, 1.5 mmol). The system was then evacuated and flushed with argon. Nitrogen-bubbled triethylamine (185 mL) and iodobenzene (12.5 mL, 112 mmol) was subsequently added via syringe, and the solution was allowed to stir at room temperature overnight under an argon atmosphere. The resulting mixture was quenched with addition of saturated NH₄Cl solution, extracted with ethyl acetate and brine. The combined organic phase was dried with MgSO₄ and concentrated through rotary evaporation. The crude product was ultimately purified with column chromatography on silica gel (ethyl acetate/hexane = 1:4) to give the title compound 4 as a pale-yellow solid (13.5 g, 38 mmol, 51%). ¹H NMR (400 MHz, CDCl₃) δ 7.88 – 7.81 (m, 1H), 7.56 – 7.49 (m, 1H), 7.44 – 7.35 (m, 5H), 7.33 – 7.27 (m, 5H), 7.25 – 7.17 (m, 2H), 5.36 (q, *J* = 3.5 Hz, 1H), 3.13 (d, *J* = 6.3 Hz, 2H), 2.48 (d, *J* = 3.5 Hz, 1H), 2.44 (s, 3H). ¹³C NMR (101 MHz, CDCl₃) δ 136.97, 136.56, 136.50, 131.67, 130.16, 128.22, 127.92, 126.87, 125.33, 124.34, 123.36, 122.64, 120.25, 119.79, 118.60, 110.77, 86.57, 83.23, 66.95, 29.32, 21.04. HRMS (*m/z*, MALDI, [M+H]⁺) calcd for C₂₅H₂₁NO 352.1701 found 352.2106. HRMS (*m/z*, MALDI, [M-OH]⁺) calcd for C₂₅H₂₁NO 334.1596 found 334.1982.

Synthesis of 3-iodo-4-phenyl-9-(*p*-tolyl)-9*H*-carbazole (PTCz-I)

To a round bottom flask was added a mixture of 4 (7.04 g, 20 mmol), potassium carbonate (2.80 g, 20 mmol), and isopropyl alcohol (400 mL). Then, iodine monochloride (3.2 mL, 60 mmol) was added dropwise via syringe, and the solution was allowed to stir at room temperature for 30 minutes. The resulting mixture was quenched with addition of saturated Na₂S₂O₃ solution, concentrated through rotary evaporation, extracted with ethyl acetate and brine. The combined organic phase was dried with MgSO₄ and concentrated through rotary evaporation. The crude product was ultimately purified with column chromatography on silica gel (dichloromethane/hexane = 1:4) to give the title compound PTCz-I as a white solid (8.16 g, 17.8 mmol, 89%). ¹H NMR (400 MHz, CDCl₃) δ 7.89 (d, *J* = 8.7 Hz, 1H), 7.65 – 7.55 (m, 3H), 7.44 – 7.37 (m, 6H), 7.33 – 7.27 (m, 2H), 7.12 (d, *J* = 8.7 Hz, 1H), 6.94 (ddd, *J* = 8.1, 5.0, 3.3 Hz, 1H), 6.68 (dt, *J* = 8.0, 1.0 Hz, 1H), 2.50 (s, 3H). ¹³C NMR (101 MHz, CDCl₃) δ 143.45, 141.17, 141.10, 140.92, 137.94, 135.21, 134.41, 130.61, 129.23, 128.85, 128.11, 127.18, 126.13, 122.87, 122.42, 122.29, 119.83, 110.83, 109.59, 89.17, 21.26. HRMS (*m/z*, MALDI, [M]⁺) calcd for C₂₅H₁₈NI 459.0484 found 459.0501.

Synthesis of 4-phenyl-9-(*p*-tolyl)-9*H*-3,9'-bicarbazole (PTCz-9'Cz)

To a sealed tube was added PTCz-I (400 mg, 0.87 mmol), carbazole (174.6 mg, 1.04 mmol), and copper(I) oxide (203.3 mg, 1.42 mmol). The tube was evacuated, flushed with argon, and added *N,N*-dimethylacetamide (DMAc, 1.0 mL) via syringe. The mixture was then heated to 190°C and reacted overnight. The resulting solution was passed through a celite pad, washed with dichloromethane, dried over MgSO₄ and concentrated through rotary evaporation. The crude product was purified with column chromatography on silica gel (dichloromethane/hexane = 1:4) to give the title compound PTCz-9'Cz as a white solid (290 mg, 0.58 mmol, 67%). ¹H NMR (400 MHz, CDCl₃) δ 8.01 (dt, *J* = 7.8, 1.0 Hz, 2H), 7.55 – 7.52 (m, 2H), 7.48 (dd, *J* = 7.9, 5.7 Hz, 3H), 7.42 – 7.35 (m, 3H), 7.33 – 7.28 (m, 4H), 7.17 (ddd, *J* = 7.9, 7.2, 1.0 Hz, 2H), 7.13 (d, *J* = 0.9 Hz, 1H), 7.12 – 7.06 (m, 5H), 2.53 (s, 3H). ¹³C NMR (101 MHz, CDCl₃) δ 142.64, 141.98, 141.16, 138.05, 137.47, 136.37, 134.57, 130.68, 128.70, 127.94, 127.66, 127.39, 127.17, 126.14, 125.39, 122.89, 122.66, 122.45, 119.88, 118.97, 110.13, 110.03, 109.86, 21.29. HRMS (*m/z*, MALDI, [M]⁺) calcd for C₃₇H₂₆N₂ 498.2096, found 498.2108.

Synthesis of 4-phenyl-9,9'-di-*p*-tolyl-9*H*,9'*H*-3,3'-bicarbazole (PTCz-3'TCz)

To a double-necked flask was added a mixture of PTCz-I (2.33 g, 5.08 mmol), (9-phenyl-9*H*-carbazol-3-yl)boronic acid (1.40 g, 4.80 mmol), 3-(4,4,5,5-tetramethyl-1,3,2-dioxaborolan-2-yl)-9-(*p*-tolyl)-9*H*-carbazole (2.92 g, 7.62 mmol), tetrakis(triphenylphosphine)palladium(0) (587 mg, 0.508 mmol), tri-*tert*-butylphosphonium tetrafluoroborate (589 mg, 2.03 mmol), and potassium carbonate (4.21 g, 30.5 mmol). The system was then evacuated and flushed with argon. Anhydrous toluene (175 mL) and nitrogen-bubbled ethanol/deionized water = 1:1 (76 mL) was added via syringe, and the solution was allowed to stir at 100°C overnight under an argon atmosphere. The resulting mixture was concentrated through rotary evaporation, extracted with CH₂Cl₂ and water, dried over MgSO₄ and concentrated to give the crude product, which was then purified with column chromatography on silica gel (dichloromethane/hexane = 1:4) to afford the title compound PTCz-3'TCz as a white solid (1.00 g, 1.5 mmol, 75%). ¹H NMR (400 MHz, CD₂Cl₂) δ 8.06 – 7.95 (m, 2H), 7.63 – 7.58 (m, 1H), 7.53 – 7.39 (m, 12H), 7.39 – 7.16 (m, 9H), 6.95 – 6.84 (m, 2H), 2.52 (s, 3H), 2.47 (s, 3H). ¹³C NMR (101 MHz, CD₂Cl₂) δ 142.32, 141.78, 140.93, 140.82, 139.89, 138.41, 137.99, 136.14, 135.48, 135.39, 134.25, 134.22, 131.12, 131.10, 130.95, 129.30, 129.28, 128.84, 127.78, 127.61, 127.24, 126.32, 126.10, 123.87, 123.83, 123.28, 122.91, 122.49, 122.34, 120.56, 120.22, 119.86, 110.31, 110.08, 109.34, 109.17, 21.57, 21.49. HRMS (*m/z*, MALDI, [M]⁺) calcd for C₄₄H₃₂N₂ 588.2565, found 588.2589.

Synthesis of 4-phenyl-*N,N*,9-tri-*p*-tolyl-9*H*-carbazol-3-amine (PTCz-NTol₂)

To a sealed tube was added PTCz-I (1.2 g, 2.6 mmol), di-*p*-tolylamine (618.5 mg, 3.14 mmol), and copper(I) oxide (609.3 mg, 4.26 mmol). The tube was evacuated, flushed with argon, and added *N,N*-dimethylacetamide (DMAc, 3.0 mL) via syringe. The mixture was then heated to 190°C and reacted overnight. The resulting solution was passed through a celite pad, washed with dichloromethane, dried over MgSO₄ and concentrated through rotary evaporation. The crude product was purified with column chromatography on silica gel (dichloromethane/hexane = 1:9) to give the title compound PTCz-NTol₂ as a light-yellow solid (412 mg, 0.78 mmol, 30%). ¹H NMR (400 MHz, CDCl₃) δ 7.48 (d, *J* = 8.4 Hz, 2H), 7.44 – 7.39 (m, 2H), 7.37 (s, 2H), 7.33 – 7.26 (m, 2H), 7.26 – 7.18 (m, 3H), 7.17 – 7.10 (m, 2H), 6.90 (qq, *J* = 2.9, 1.3 Hz, 2H), 6.87 – 6.82 (m, 4H), 6.74 – 6.66 (m, 4H), 2.51 (s, 3H), 2.23 (s, 6H). ¹³C NMR (101 MHz, CDCl₃) δ 146.18, 141.62, 139.32, 137.92, 137.69, 137.61, 136.38, 134.82, 130.52, 129.64, 129.22, 129.04, 128.10, 127.98, 127.91, 127.24, 126.96, 125.58, 123.10, 122.89, 122.33, 121.30, 120.59, 119.47, 116.71, 110.10, 109.57, 21.25, 20.59. HRMS (m/z, MALDI, [M]⁺) calcd for C₃₉H₃₂N₂ 528.2565, found 528.2582.

Synthesis of 5,10-bis(9-phenyl-9*H*-carbazol-3-yl)naphtho[1,2-*c*:5,6-*c'*]bis([1,2,5]thiadiazole) (iCzPNT)

To a double-necked flask was added a mixture of 5,10-dibromonaphtho[1,2-*c*:5,6-*c'*]bis([1,2,5]thiadiazole) (0.80 g, 2 mmol), (9-phenyl-9*H*-carbazol-3-yl)boronic acid (1.44 g, 5 mmol), tetrakis(triphenylphosphine)palladium(0) (0.23 g, 0.2 mmol), and potassium carbonate (1.66 g, 12 mmol). The system was then evacuated and flushed with argon. Anhydrous toluene (48 mL) and nitrogen-bubbled deionized water (6 mL) was added via syringe, and the solution was allowed to stir at 110°C for 48 hours under an argon atmosphere. The resulting mixture was concentrated through rotary evaporation, dissolved in CHCl₃ and washed with brine. The combined organic phase was dried over MgSO₄ and concentrated to give the crude product, which was then purified via Soxhlet extraction with CHCl₃ to afford the title compound iCzPNT as a red solid. (0.91 g, 1.25 mmol, 63%). ¹H NMR (400 MHz, CDCl₃) δ 9.18 (s, 2H), 8.95 (d, *J* = 1.7 Hz, 2H), 8.31 (d, *J* = 7.8 Hz, 2H), 8.24 (dd, *J* = 8.5, 1.8 Hz, 2H), 7.71 – 7.64 (m, 8H), 7.63 (d, *J* = 8.6 Hz, 2H), 7.52 (d, *J* = 3.8 Hz, 2H), 7.48 (d, *J* = 3.9 Hz, 4H), 7.39 – 7.34 (m, 2H). HRMS (m/z, MALDI, [M]⁺) calcd for C₄₆H₂₆N₆S₂ 726.1660, found 726.1623. The ¹³C NMR data of iCzPNT is not available due to poor solubility.

Synthesis of 1,3-bis(9-phenyl-9*H*-carbazol-3-yl)benzo[*c*]thiophene-5,6-dicarbonitrile (iCzBTh2CN)

To a double-necked flask was added a mixture of 1,3-dibromobenzo[*c*]thiophene-5,6-

dicarbonitrile (0.68 g, 2.00 mmol), (9-phenyl-9*H*-carbazol-3-yl)boronic acid (1.40 g, 4.80 mmol), tetrakis(triphenylphosphine)palladium(0) (0.23 g, 0.20 mmol), and potassium carbonate (1.1 g, 8.00 mmol). The system was then evacuated and flushed with argon. Anhydrous toluene (30.0 mL) and nitrogen-bubbled deionized water (7.5 mL) was added via syringe, and the solution was allowed to stir at 110°C for 24 hours under an argon atmosphere. The resulting mixture was concentrated through rotary evaporation, extracted with CH₂Cl₂ and water, dried over MgSO₄ and concentrated to give the crude product, which was then purified with column chromatography on silica gel (dichloromethane/hexane = 1:1) to afford the title compound iCzBTh2CN as an orange solid (1.00 g, 1.5 mmol, 75 %). ¹H NMR (400 MHz, CDCl₃) δ 8.38 (q, J = 1.5 Hz, 4H), 8.25 (d, J = 7.7 Hz, 2H), 7.70 – 7.64 (m, 6H), 7.64 – 7.58 (m, 5H), 7.57 – 7.51 (m, 3H), 7.51 – 7.43 (m, 4H), 7.42 – 7.34 (m, 2H). ¹³C NMR (101 MHz, CDCl₃) δ 141.60, 141.49, 141.20, 137.10, 133.80, 131.97, 131.59, 130.11, 128.42, 128.03, 127.24, 127.11, 126.95, 124.40, 123.47, 122.81, 121.29, 120.68, 116.78, 110.92, 110.42, 110.25, 109.95, 106.66. HRMS (m/z, MALDI, [M]⁺) calcd for C₄₆H₂₆N₄S 666.1878 found 666.1901.

Theoretical Calculation

Theoretical calculations with density functional theory (DFT) were conducted in the gaseous state at the B3LYP/6-31+G(d,p) level through Taiwania 1, built by the National Applied Research Laboratories, Taiwan.

Material Characterization

Thermogravimetric analysis (TGA) and differential scanning calorimetry (DSC) were conducted under a nitrogen atmosphere at a heating rate of 10 °C/min on a platinum pan via a TA Instruments Q500 TGA (V20.13 Build 39) and Netzsch 204 F1. NMR spectra were measured in CDCl₃ or CD₂Cl₂ using Varian (Utility 400) spectrometer for ¹H NMR (400 MHz) and ¹³C NMR (101 MHz). Steady-state UV-visible absorption spectra in solution were characterized by a UV-vis-NIR spectrophotometer (UV-1650 PC, Shimadzu) and in solid film were recorded by a Thermo spectrophotometer (Evo 201). Photoluminescence (PL) spectra, and phosphorescence spectra were characterized by a spectrofluorimeter (FluoroMax-P, Horiba Jobin Yvon Inc.). The time-resolved studies were performed using a time-correlated single photon counting (TCSPC) system (TimeHarp 260, PicoQuant) with the pulse LED at 285 nm (PLS280, PicoQuant) as the photoexcitation light source. PLQYs of thin films were determined using quantum yield spectrometer (Hamamatsu C9920-02). The experimental values of HOMO levels in solid state were determined with a Riken AC-2 photoemission spectrometer (PES). All the mass spectra were

recorded by the National Taiwan University Mass Spectrometry-based Proteomics Core Facility by Bruker Daltonics Autoflex speed in MALDI-TOF mode.

Cyclic voltammetry

The electrochemical properties were measured by cyclic voltammetry (CHI619B potentiostat). A glassy carbon electrode was used as a working electrode, and a platinum wire was used as a counter electrode. The oxidation potentials were conducted in dried dichloromethane (1.0 mM) with 0.1 M tetrabutylammonium hexafluorophosphate (${}^n\text{Bu}_4\text{NPF}_6$) as the supporting electrolyte. All the potentials were recorded versus Ag/AgCl as a reference electrode, further calibrated with the ferrocene/ferrocenium (Fc/Fc^+) redox couple (0.48 eV in dichloromethane/ ${}^n\text{Bu}_4\text{NPF}_6$). All the mass spectra were recorded by the National Taiwan University Mass Spectrometry-based Proteomics Core Facility by Bruker Daltonics Autoflex speed in MALDI-TOF mode.

Time-of-flight (TOF) mobility measurements

Carrier-transport properties were studied by the time-of-flight (TOF) transient photocurrent technique in the structure: ITO glass/ PTCz-9'Cz (1.06 μm), PTCz-3'TCz (1.16 μm) or PTCz-NTol₂ (1.04 μm)/Ag (200 nm), which were then placed inside a cryostat and kept under vacuum. The thickness of organic film was monitored in situ with a quartz sensor and calibrated by a thin film thickness measurement. A pulsed nitrogen laser (337 nm) was used as the excitation light source through the transparent electrode (ITO) inducing photogeneration of a thin sheet of excess carriers. Under an applied dc bias, the transient photocurrent was swept across the bulk of the organic film toward the collection electrode (Ag), and then recorded with a digital storage oscilloscope. Depending on the polarity of the applied bias, selected carriers (holes or electrons) are swept across the sample with a transit time of t_T . With the applied bias V and the sample thickness D , the applied electric field $E = V/D$, and the carrier mobility is then given by $\mu = D/(t_T E) = D^2/(V t_T)$, in which the carrier transit time, t_T , can be extracted from the intersection of two asymptotes to the tail and plateau sections in the double logarithmic plots.

Device fabrication

All chemicals were purified through vacuum sublimation prior to use. The OLEDs were fabricated through vacuum deposition of the materials at 10^{-6} Torr onto the ITO-coated glass substrates having a sheet resistance of $15 \Omega \text{ sq}^{-1}$. Prior to use the ITO surface was cleaned ultrasonically; i.e. with acetone, methanol, and deionized water in sequence and finally with UV-ozone. The deposition rate of each organic material was ca. $1\text{--}2 \text{ \AA s}^{-1}$. The $J\text{--}V\text{--}L$ characteristics of the devices were measured simultaneously in a

glovebox. A programmable source measurement unit (2614B, Keithley) was used as a driving source of the device while the light intensity was measured by a calibrated silicon detector according to standard procedures⁷. The luminance was confirmed with a spectroradiometer (TOPCON BM-9A) in the visible region. EL spectra were measured using a photodiode array (Ocean Optics USB2000+).

Tables and Figures

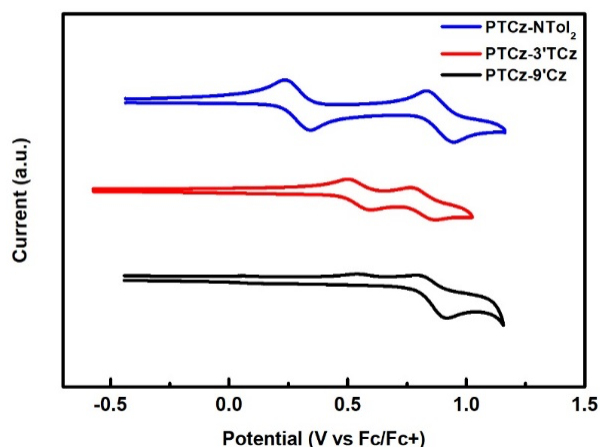


Figure S1 Cyclic voltammograms of PTCz-9'Cz, PTCz-3'TCz, and PTCz-NTol₂.

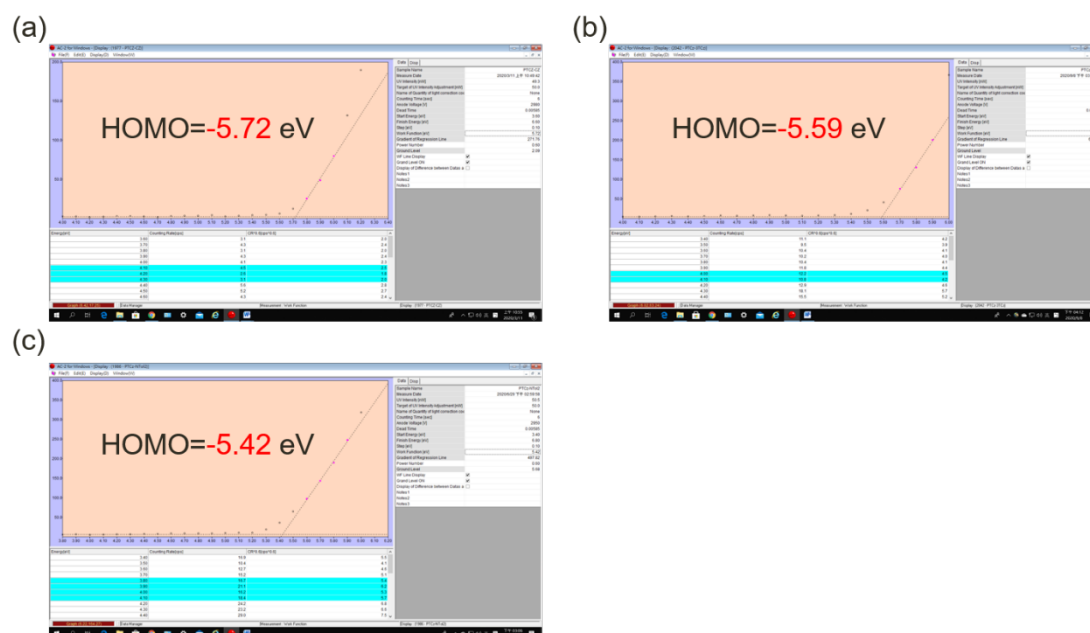


Figure S2 HOMO energy levels of (a) PTCz-9'Cz, (b) PTCz-3'TCz and (c) PTCz-NTol₂ determined by photoelectron yield spectroscopy (Riken AC-2).

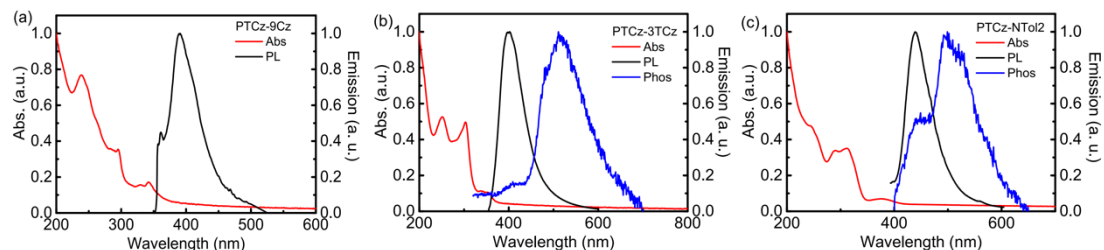


Figure S3 Room temperature absorption (UV-Vis), emission (PL) and Phosphorescence (Phos) spectra of (a) PTCz-9'Cz, (b) PTCz-3'TCz, and (c) PTCz-NTol₂ neat films.

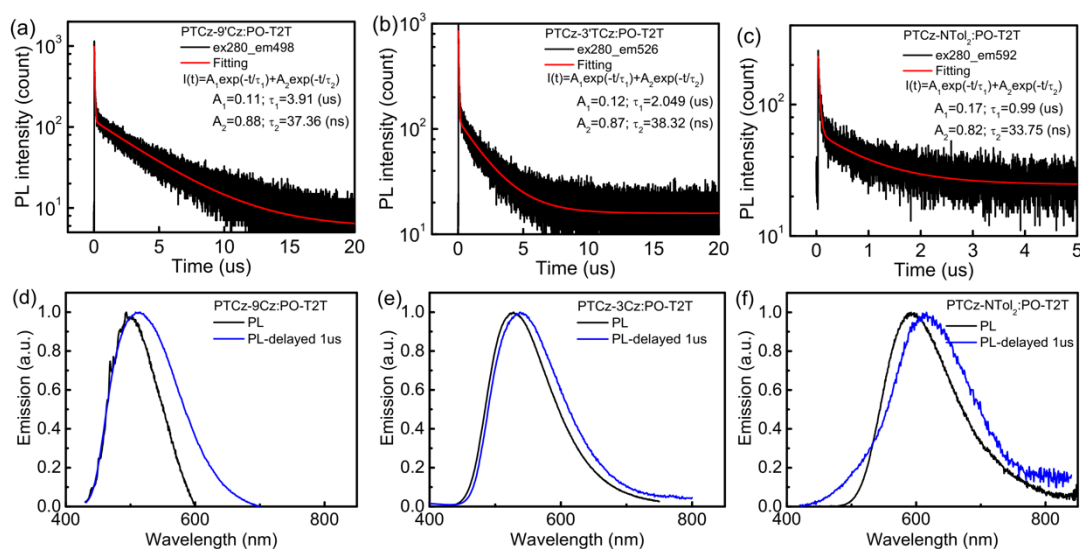


Figure S4 (a)-(c) Transient PL decays and (d)-(f) PL spectra of Donor:PO-T2T (1:1) blend films at room temperature.

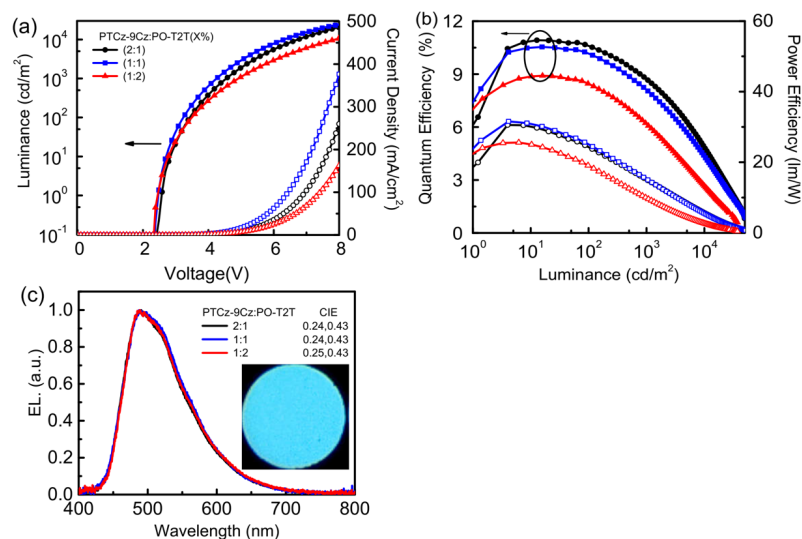


Figure S5 Plots of (a) J-V-L characteristics, (b) correlation profile of luminance with EQE and power efficiency (PE), and (c) normalized EL spectra for PTCz-9'Cz:PO-T2T devices with different donor-acceptor ratios.

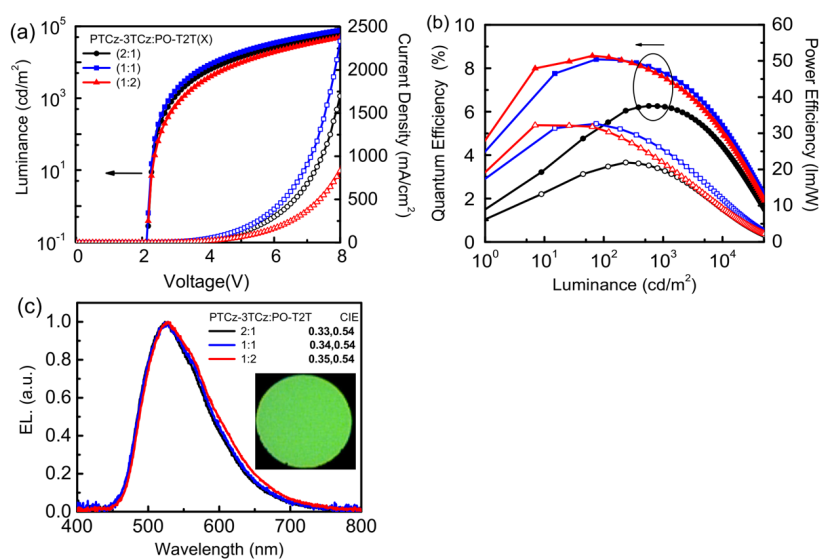


Figure S6 Plots of (a) J-V-L characteristics, (b) correlation profile of luminance with EQE and power efficiency (PE), and (c) normalized EL spectra for PTCz-3TCz:PO-T2T devices with different donor-acceptor ratios.

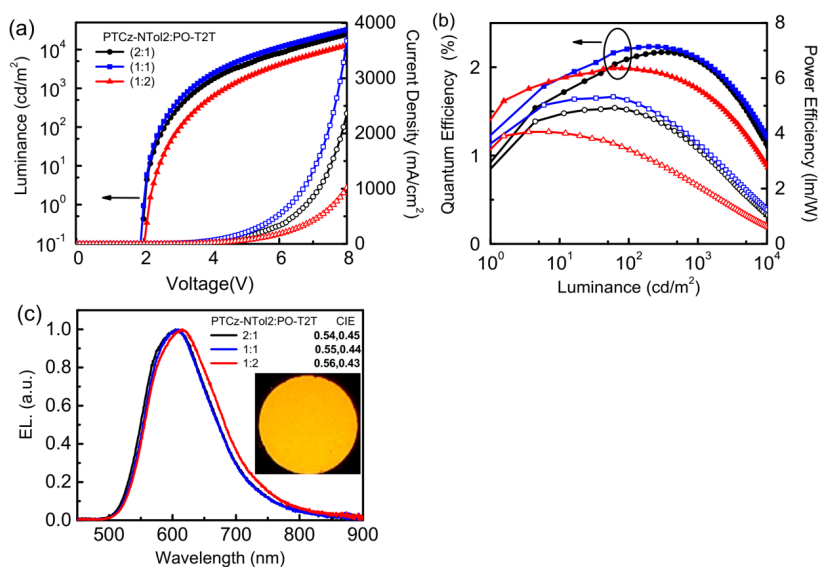


Figure S7 Plots of (a) J-V-L characteristics, (b) correlation profile of luminance with EQE and power efficiency (PE), and (c) normalized EL spectra for PTCz-NTol₂:PO-T2T devices with different donor-acceptor ratios.

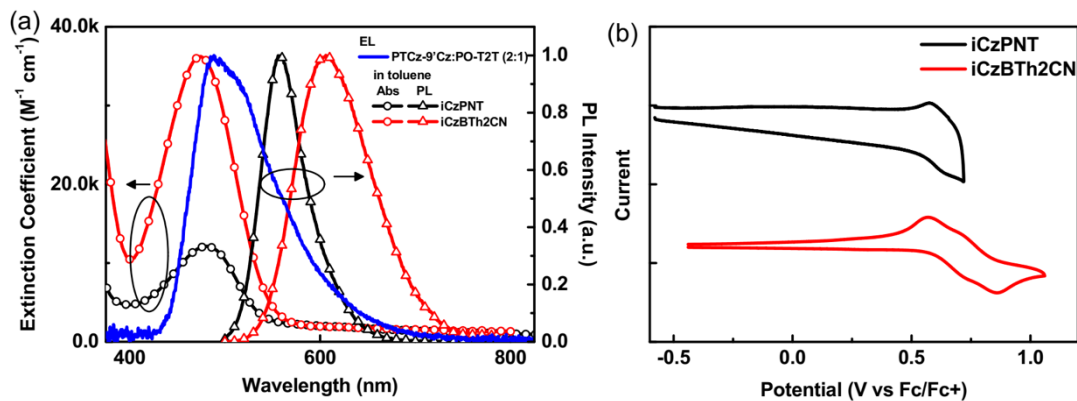


Figure S8 (a) Room temperature absorption (UV-Vis) and emission (PL) spectra of iCzPNT and iCzBTh2CN in toluene solution and (b) cyclic voltammograms of iCzPNT and iCzBTh2CN. The cyclic voltammogram of iCzPNT was obtained despite poor solubility in CH_2Cl_2 .

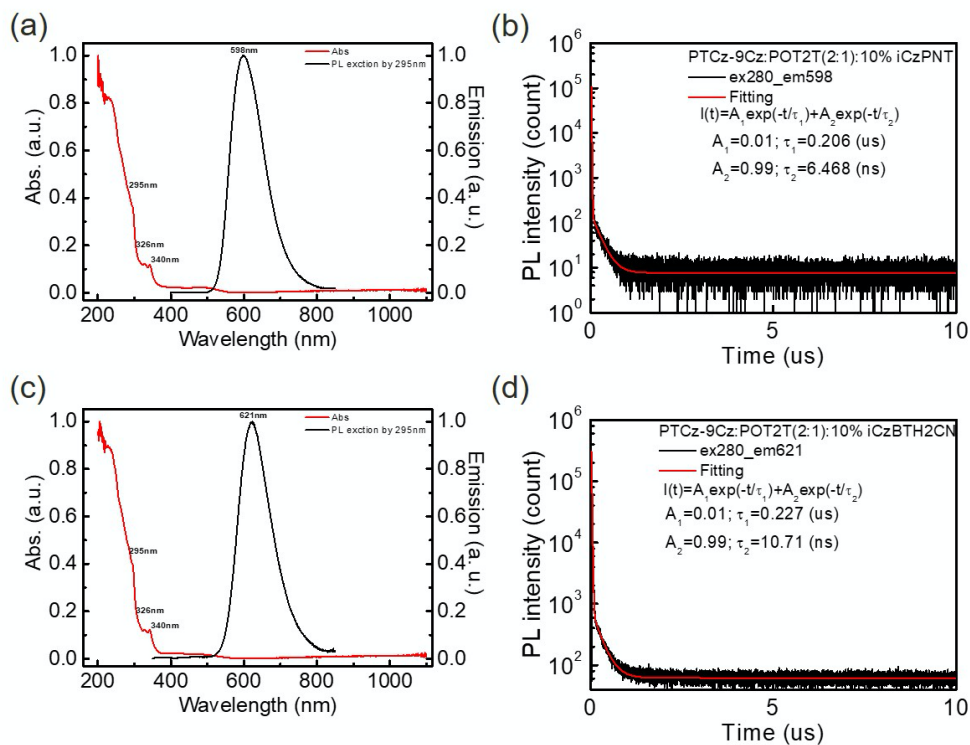


Figure S4 Room temperature absorption (UV-Vis) and emission (PL) spectra of PTCz-9Cz:PO-T2T (2:1) blend films with 10 wt%-doped (a) iCzPNT and (c) iCzBTh2CN and transient PL decays of PTCz-9Cz:PO-T2T (2:1) blend films with 10 wt%-doped (b) iCzPNT and (d) iCzBTh2CN at room temperature.

Table S1 Theoretical calculations of PTCz-based donors (a) LUMO (b) HOMO and (c) ground state geometry at the B3LYP/6-31+G(d,p) level

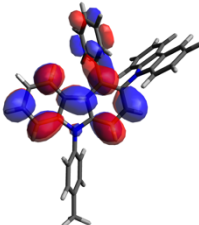
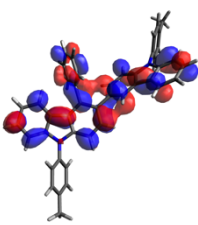
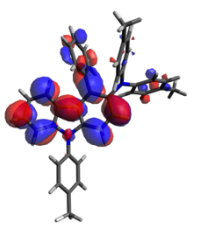
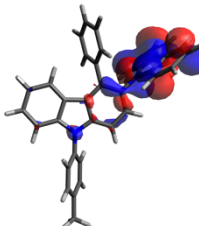
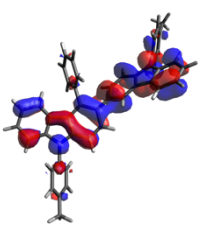
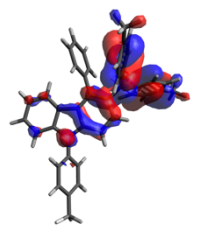
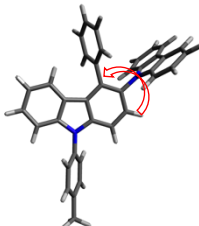
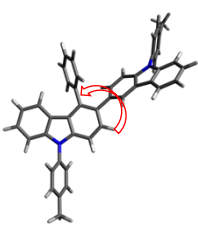
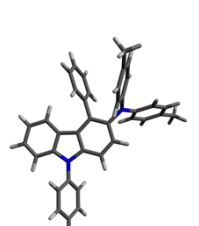
| | PTCz-9'Cz | PTCz-3'TCz | PTCz-NTol ₂ |
|-----|---|---|---|
| (a) |  -1.28 eV |  -1.08 eV |  -1.12 eV |
| (b) |  -5.47 eV |  -5.23 eV |  -4.87 eV |
| (c) |  83° |  57° |  |

Table S2 Theoretical calculations of TCz-based donors (a) LUMO (b) HOMO and (c) ground state geometry at the B3LYP/6-31+G(d,p) level

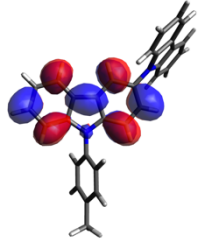
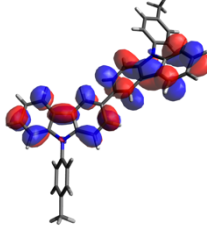
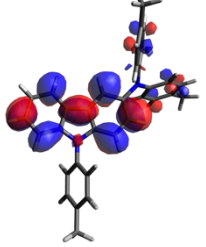
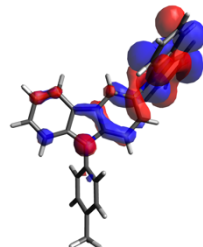
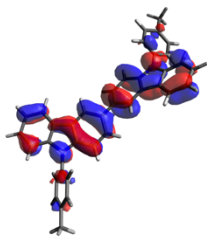
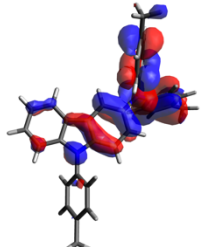
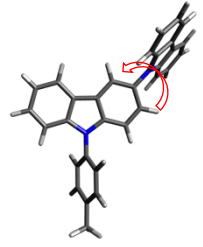
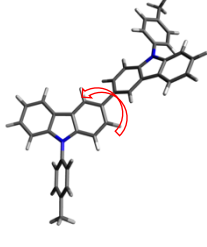
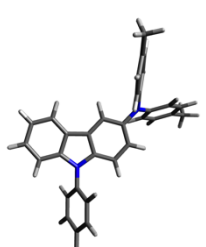
| | TCz-9'Cz | TCz-3'TCz | TCz-NTol ₂ |
|-----|---|---|---|
| (a) |  -1.30 eV |  -1.01 eV |  -1.13 eV |
| (b) |  -5.44 eV |  -5.19 eV |  -4.81 eV |
| (c) |  69° |  41° |  |

Table S3 Physical properties of iCzPNT and iCzBTh2CN.

| | λ_{abs} [nm] ^a (ϵ [M ⁻¹ cm ⁻¹]) | λ_{PL} [nm] ^a (PLQY) ^b | E_g [eV] ^c | HOMO [eV] ^d | LUMO [eV] ^e | T_d [°C] |
|-----------|---|--|----------------------------|---------------------------|---------------------------|---------------|
| iCzPNT | 480 (12114) | 560 (92%) | 2.31 | -5.32 | -3.01 | 441 |
| iCzBTh2CN | 475 (36210) | 606 (85 %) | 2.26 | -5.44 | -3.18 | 465 |

^a Measured in toluene solution (10⁻⁵ M). ^b Measured by an integrating sphere. ^c Estimated from the onset of the UV-Vis absorption curves in toluene. ^d Calculated from potential vs. ferrocene/ferrocenium redox couple. ^e Calculated from the difference between HOMO and corresponding optical bandgap.

NMR Spectra

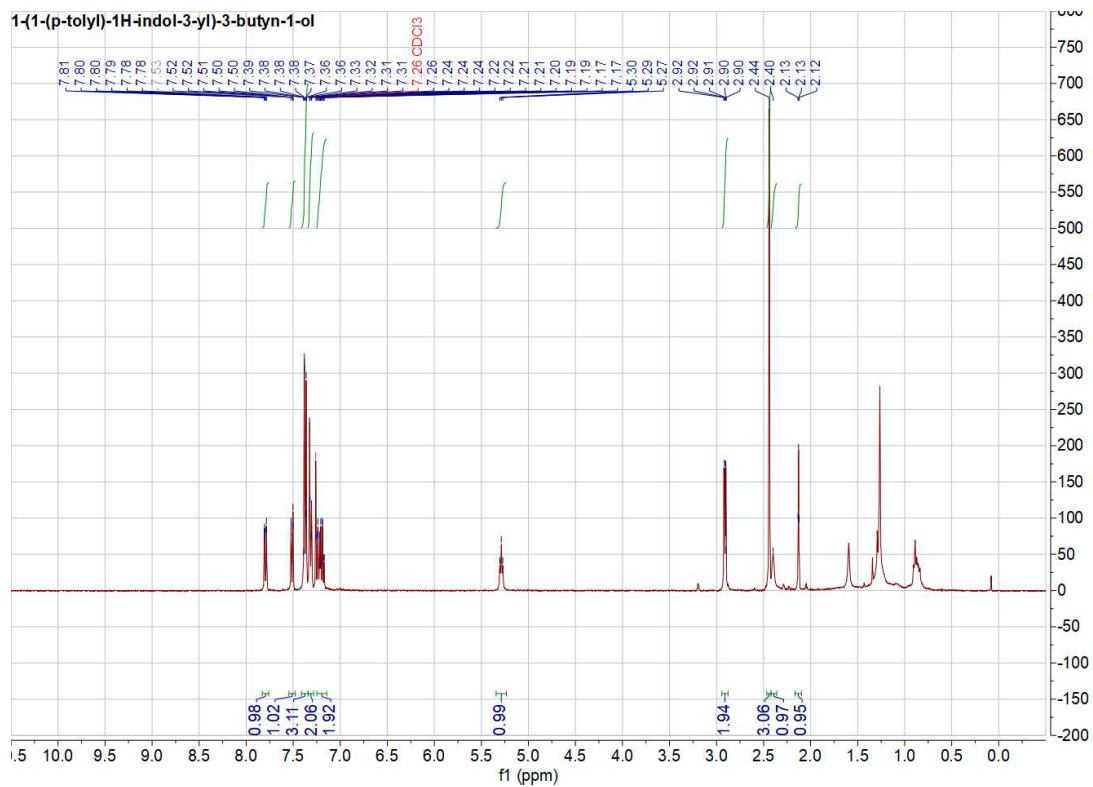


Figure S10 ¹H NMR spectrum of 3.

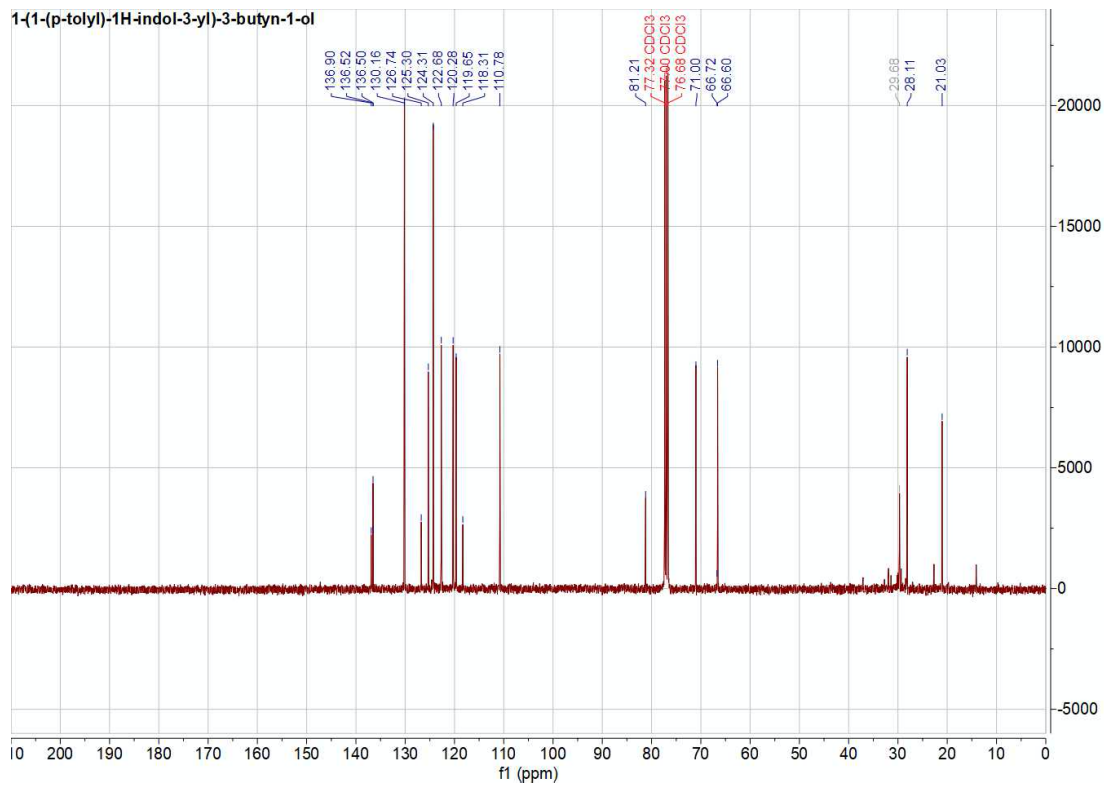


Figure S11 ¹³C NMR spectrum of 3.

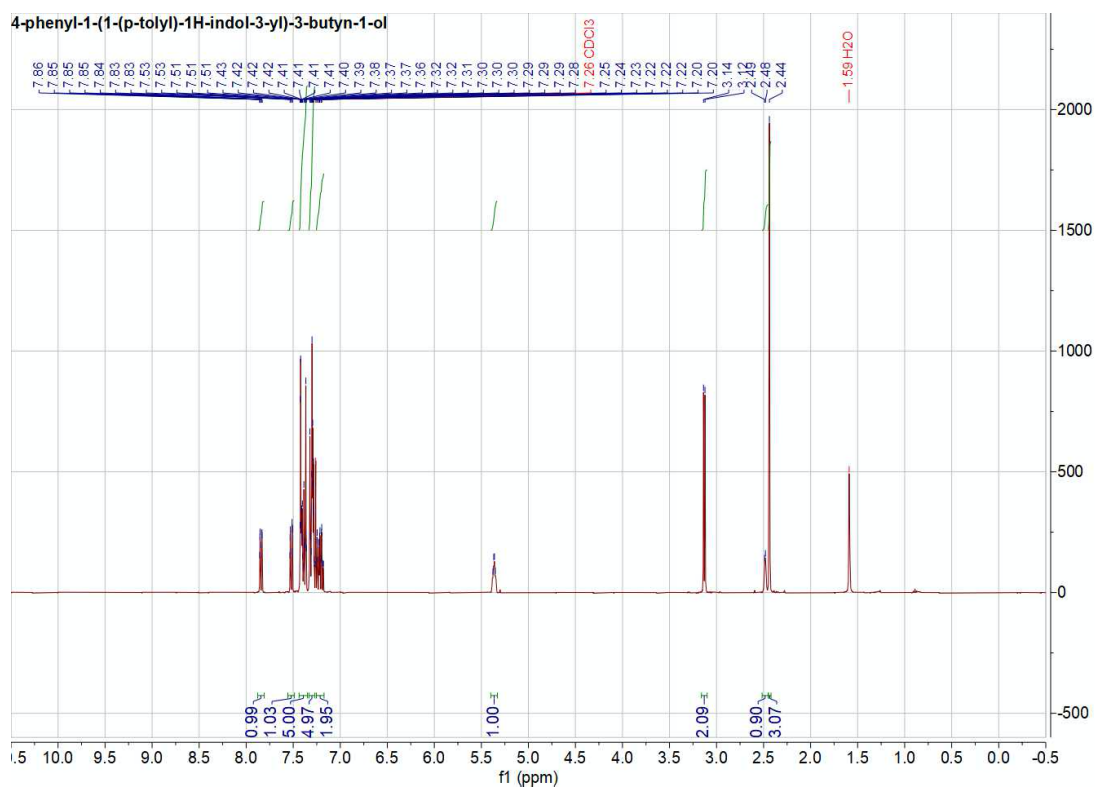


Figure S12 ¹H NMR spectrum of 4.

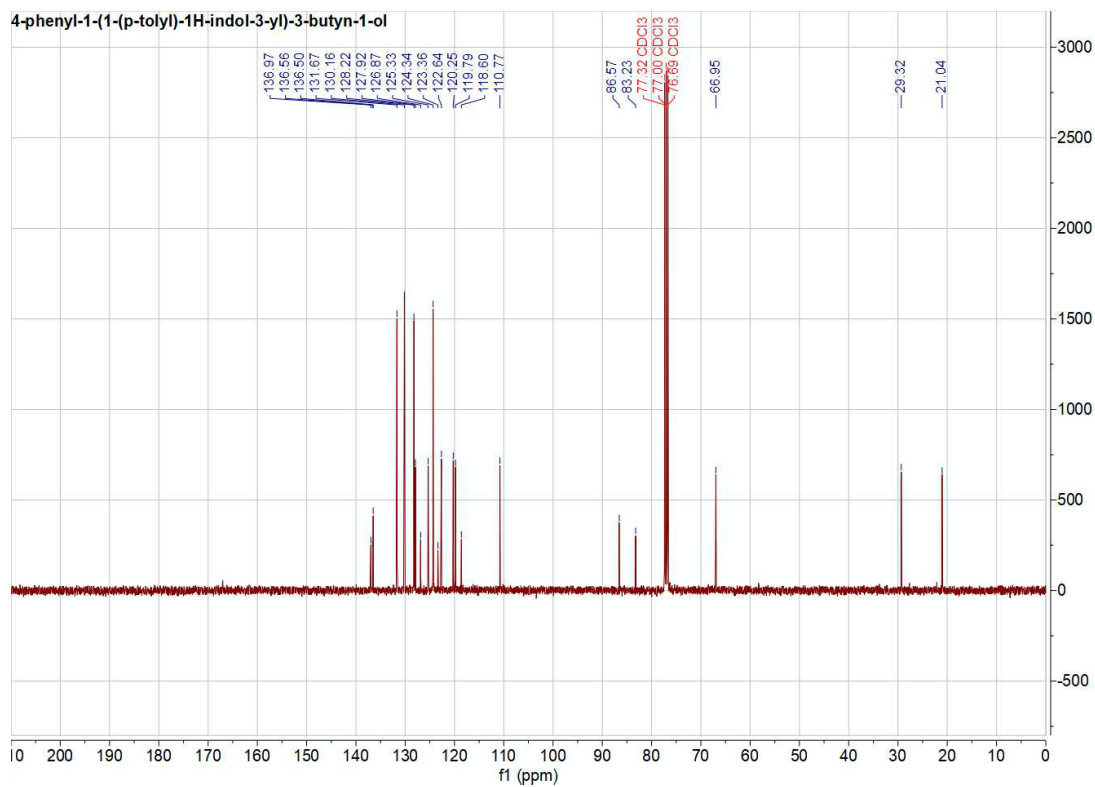


Figure S13 ¹³C NMR spectrum of 4.

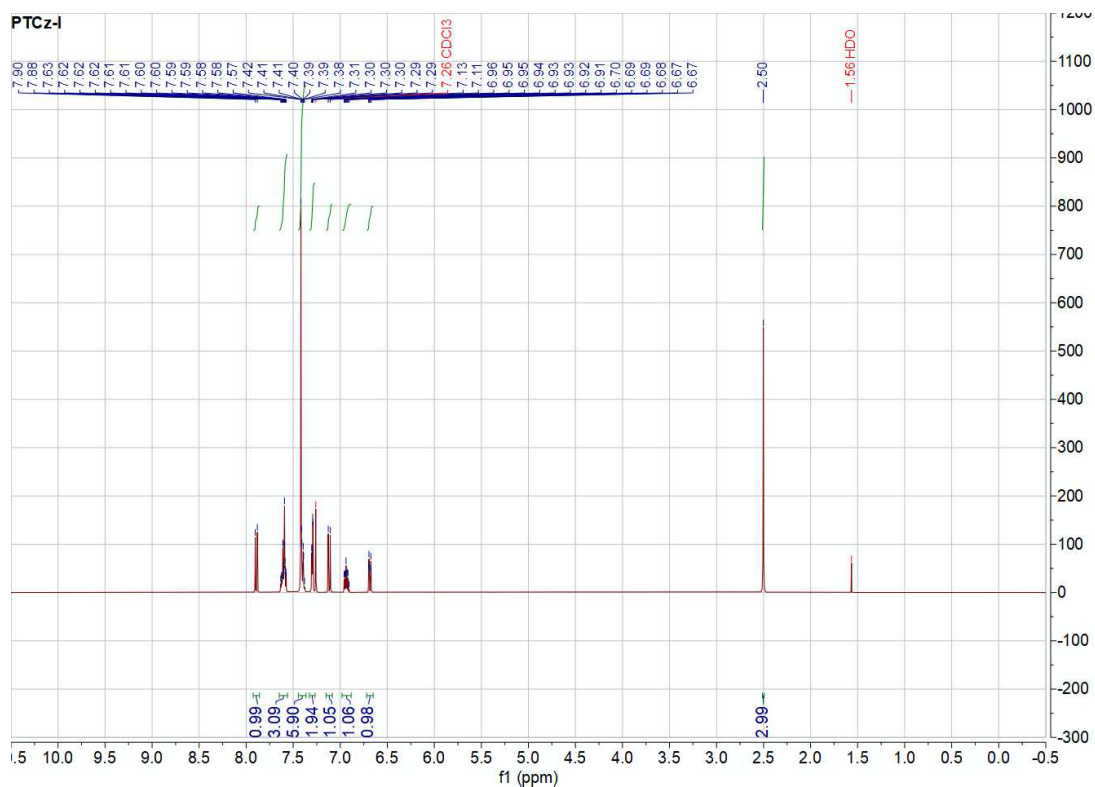


Figure S14 ¹H NMR spectrum of PTCz-I.

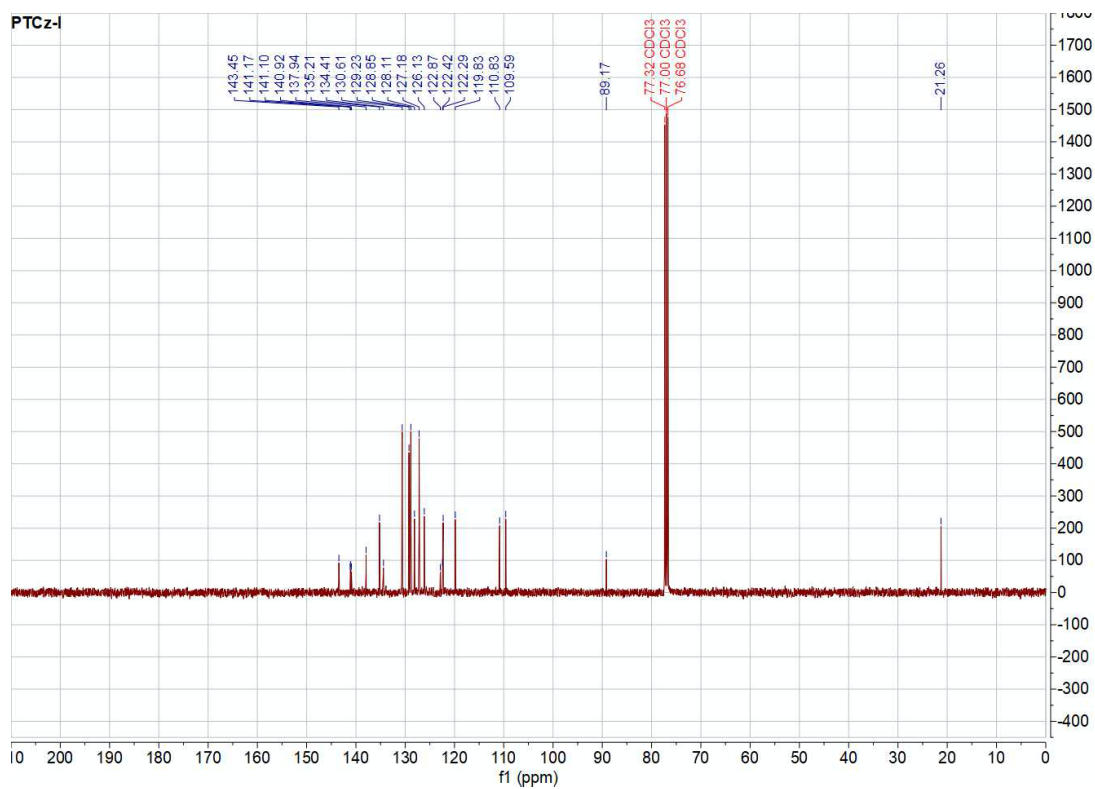


Figure S15 ¹³C NMR spectrum of PTCz-I.

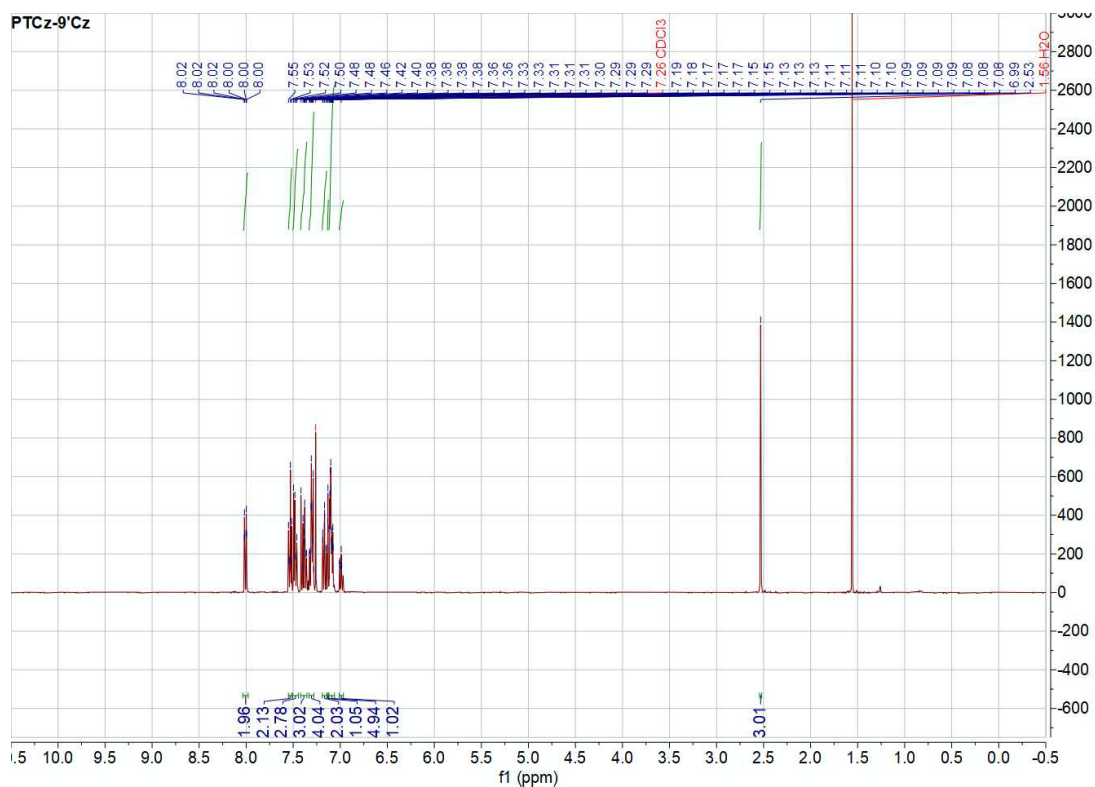


Figure S16 ^1H NMR spectrum of PTCz-9'Cz.

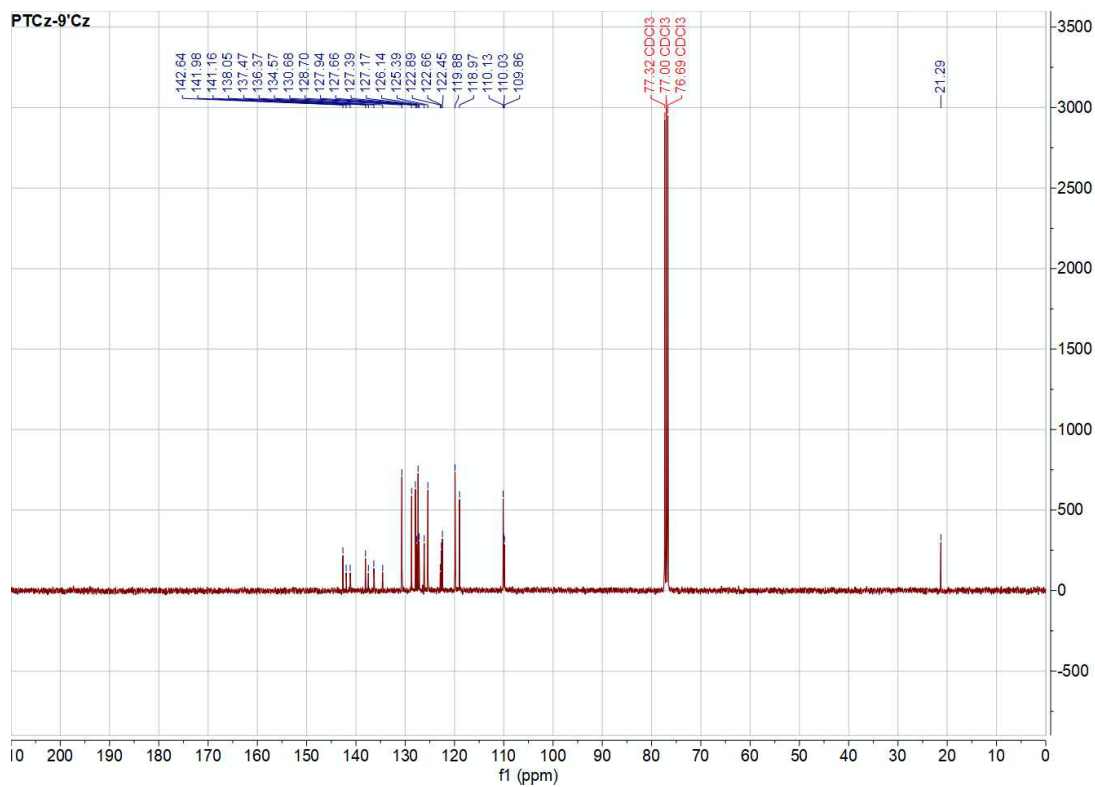


Figure S17 ^{13}C NMR spectrum of PTCz-9'Cz.

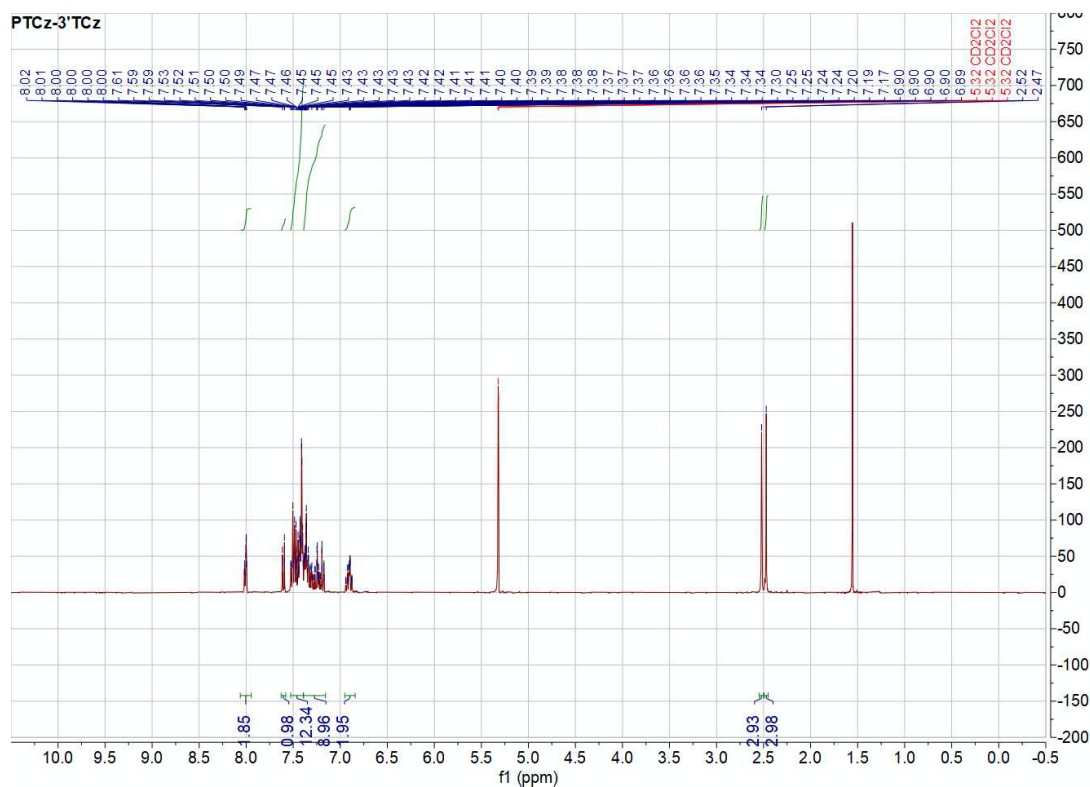


Figure S18 ^1H NMR spectrum of PTCz-3'TCz.

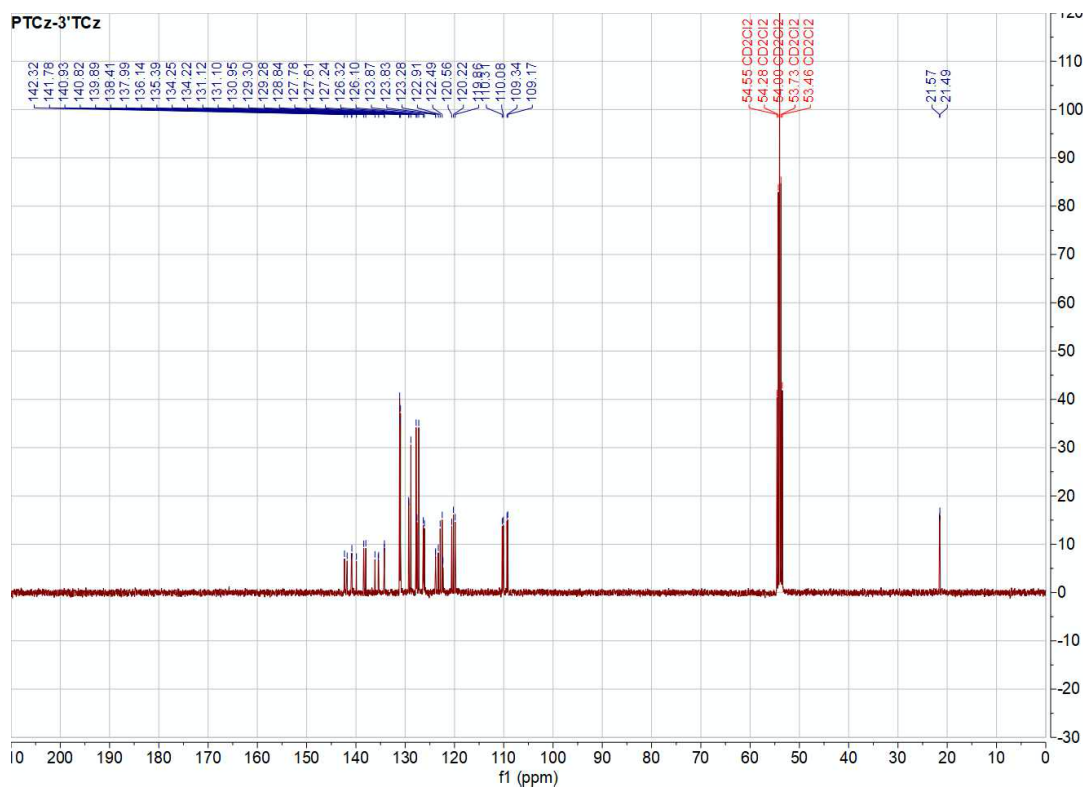


Figure S19 ^{13}C NMR spectrum of PTCz-3'TCz.

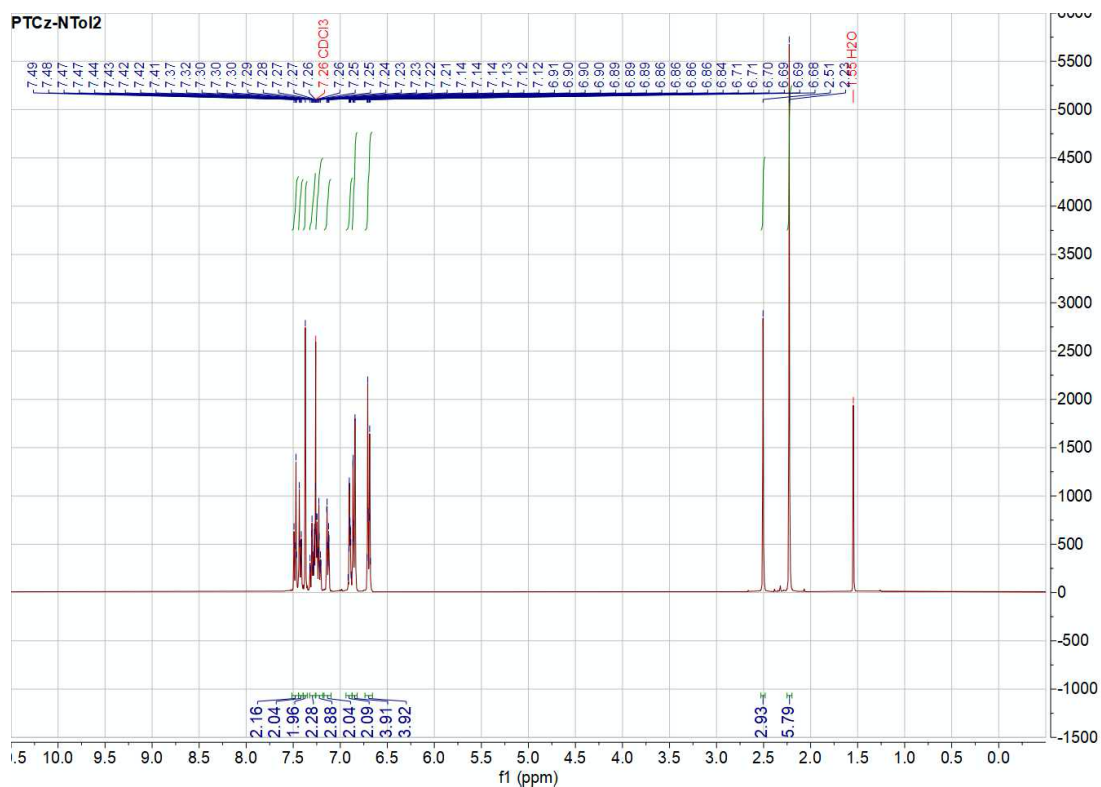


Figure S20 ¹H NMR spectrum of PTCz-NTol₂.

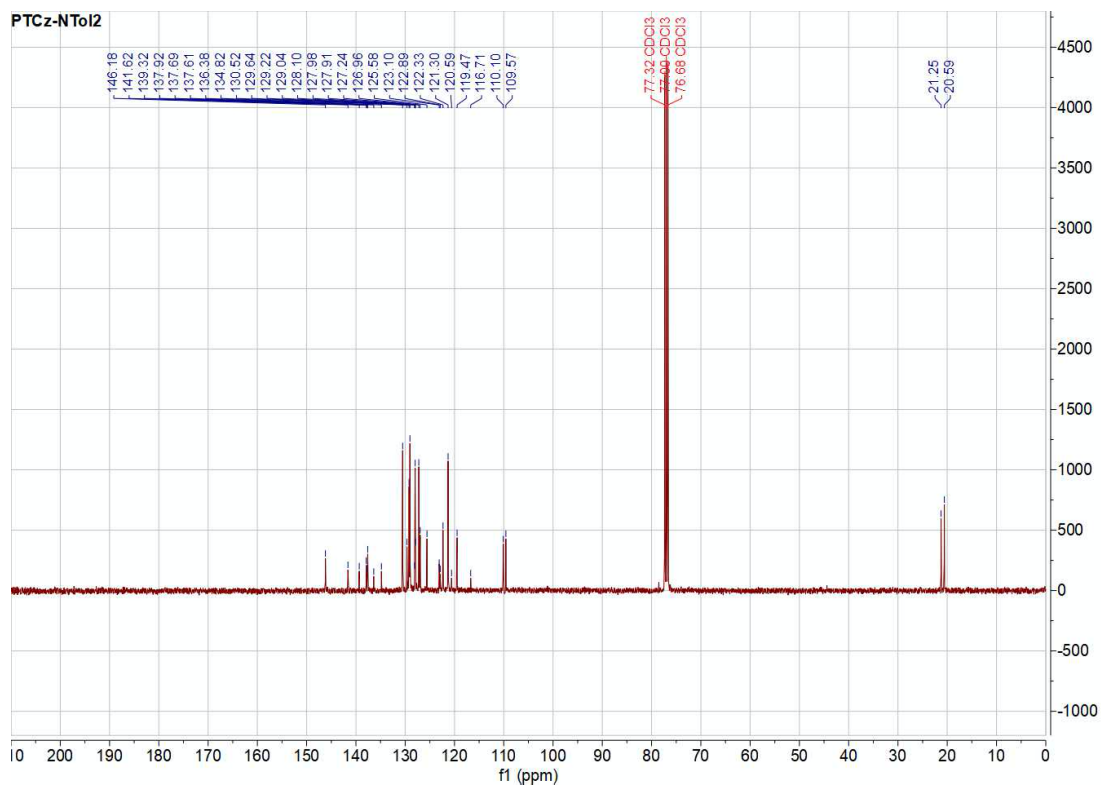


Figure S21 ¹³C NMR spectrum of PTCz-NTol₂.

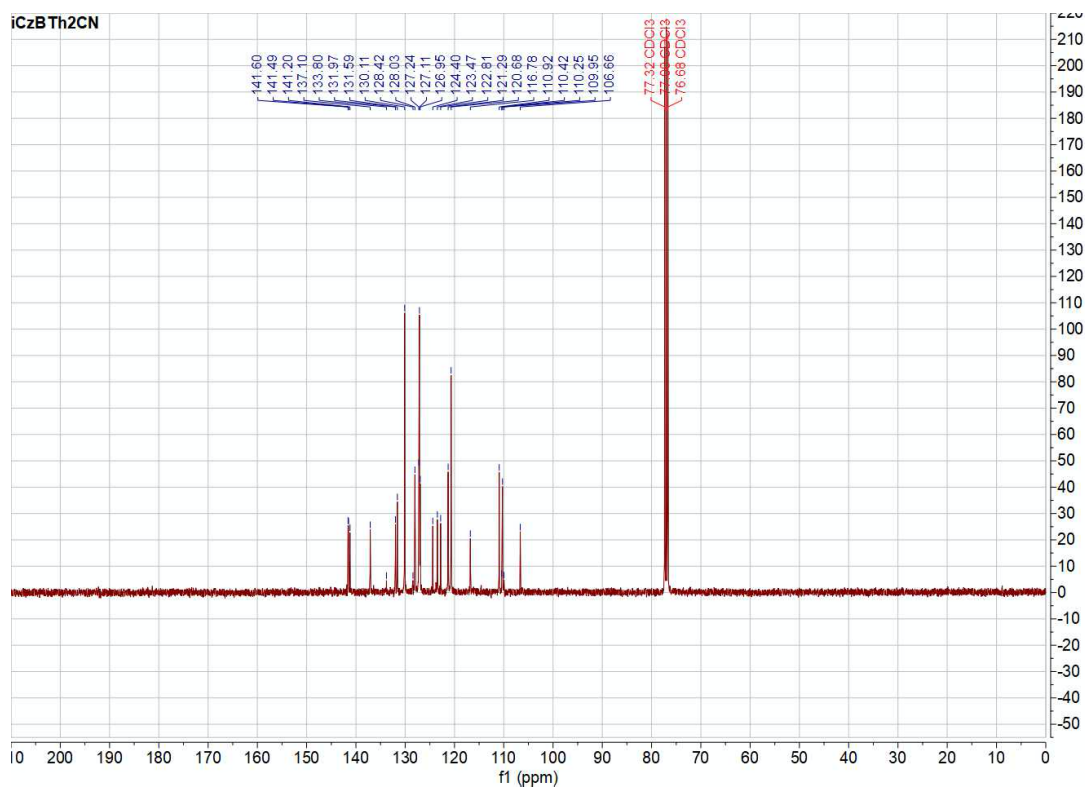


Figure S24 ¹³C NMR spectrum of iCzBTh2CN.

References

1. J. C. Antilla, A. Klapars and S. L. Buchwald, The Copper-Catalyzed N-Arylation of Indoles, *J. Am. Chem. Soc.*, 2002, 124, 11684-11688.
2. J. G. Quirrit, S. N. Lavrenov, K. Poindexter, J. Xu, C. Kyauk, K. A. Durkin, I. Aronchik, T. Tomasiak, Y. A. Solomatin, M. N. Preobrazhenskaya and G. L. Firestone, Indole-3-carbinol (I3C) analogues are potent small molecule inhibitors of NEDD4-1 ubiquitin ligase activity that disrupt proliferation of human melanoma cells, *Biochem. Pharmacol.*, 2017, 127, 13-27.
3. F. Yang, T. Yu, Y. Zhao, H. Zhang and Y. Niu, Synthesis, photoluminescence properties of novel cationic Ir(III) complexes with phenanthroimidazole derivative as the ancillary ligand, *Polyhedron*, 2017, 138, 74-81.
4. T. Higashino, Y. Kurumisawa, S. Nimura, H. Iiyama and H. Imahori, Enhanced Donor- π -Acceptor Character of a Porphyrin Dye Incorporating Naphthobisthiadiazole for Efficient Near-Infrared Light Absorption, *Eur. J. Org. Chem.*, 2018, 2018, 2537-2547.
5. J. D. Douglas, G. Griffini, T. W. Holcombe, E. P. Young, O. P. Lee, M. S. Chen and J. M. J. Fréchet, Functionalized Isothianaphthene Monomers That Promote Quinoidal Character in Donor-Acceptor Copolymers for Organic Photovoltaics, *Macromolecules*, 2012, 45, 4069-4074.
6. W.-Y. Hung, G.-C. Fang, S.-W. Lin, S.-H. Cheng, K.-T. Wong, T.-Y. Kuo and P.-T. Chou, The First Tandem, All-exciplex-based WOLED, *Sci. Rep.*, 2014, 4, 5161.
7. S. R. Forrest, D. D. C. Bradley and M. E. Thompson, Measuring the Efficiency of Organic Light-Emitting Devices, *Adv. Mater.*, 2003, 15, 1043-1048.